Materials Characterization 141 (2018) 267–278

Contents lists available at ScienceDirect

Materials Characterization

journal homepage: www.elsevier.com/locate/matchar

Non-equilibrium approach to prediction of microstructure evolution for metals undergoing severe plastic deformation

E.N. Borodin[a,*], V. Bratov[b,c]

[a] Mechanics and Physics of Solids Research Group, School of MACE, The University of Manchester, Manchester, M13 9PL, UK
[b] Institute of Problems of Mechanical Engineering RAS, 199178 V.O., Bolshoj pr., 61, St. Petersburg, Russia
[c] Saint-Petersburg State University, 199034 Universitetskaya nab., 7-9, St. Petersburg, Russia

ARTICLE INFO

Keywords:
Severe plastic deformation
Numerical simulations
Copper alloys
Microstructure evolution
Dynamic recrystallization
Dislocation density
Non-equilibrium state
FEM

ABSTRACT

Available models of dynamic recrystallization have a number of disadvantages that in most cases make them inapplicable for practical predictions of material microstructure evolution. Both the microstructural and the empirically based approaches do not reflect physical processes leading to evolution of material defect structure in the process of plastic deformation. This work presents an attempt to develop a consistent physically-based model of dynamic recrystallization. This model, accounting for physical nature of processes of material defect structure evolution, should provide a possibility to predict evolution of several different experimentally measurable parameters of material microstructure without introduction of big number of fitting parameters. It is suggested that such a model should be based on equation for evolution of fraction of high-angle grain boundaries (HAGBs) in the process of deformation. It is shown, that the new model gives a possibility to predict the evolution of dislocation cells and grain boundaries in copper-based alloys providing good coincidence with experimental observations. Full 3-dimensional numerical simulation of multidirectional forging of copper is performed utilizing the developed dynamic recrystallization model. The same 3D simulations demonstrate new noteworthy effects connected to inhomogeneous distribution of plastic strain within the bulk of the material and material strain hardening.

1. Introduction

Experimental investigations of severe plastic deformation (SPD) of different metals [1–10] show that changes obtained by different elements of material macrostructure in the process of deformation are non-monotonous and are dependent on the whole set of external factors. Among the most significant properties of microstructure modified in the process of deformation one can distinguish scalar density of dislocations inside cells and in the cell walls [1,2,4,5], average size of dislocation cells, average grain size, dispersion of grain size distribution, aspect ratio (geometrical property characterizing grain shape) of individual grains [1,2] and fraction of high angle grain boundaries (HAGBs) with misorientation angles exceeding 15° [1,2]. Some of these parameters, such as scalar density of mobile/immobile dislocations [8], average grain size and fraction of HAGBs are dynamically interconnected.

All of these parameters can be registered by a precise appraisal of microstructure, obtained by the processed metallic sample after each pass of multidirectional forging (MDF) [1,2], accumulative roll bonding (ARB) [1,3,6], high pressure torsion (HPT) [3,6,11,12] or equal-channel angular pressing (ECAP) [3,6,12], being the most common SPD-processes. A significant number of known works is devoted to investigation of the influence of parameters of microstructure on microhardness, yield stress, strength, ultimate fracture strain and other mechanical parameters of metallic materials [1,3,7,9,12,13]. It is notable that when analysing mechanical properties of the processed materials it can be observed that different SPD processes often result in very similar changes of mechanical properties for the same accumulated strain, differing only in details [1,14]. Nevertheless, these details can be essential for other material properties, such as conductivity [3,9,15], stability of the received microstructure and diffusive properties [3]. Besides, different SPD methods result in a different degree of spatial inhomogeneity of the resulting microstructure. The simplest and hence the most convenient for analysis are SPD processes of multidirectional forging (MDF) and accumulative roll bonding, implementing essentially the same modes of shear deformation. In [1,2] A. Belyakov et al. analysed dynamic recrystallization in copper and steels subjected to a different number of MDF passes. For precise analysis of the dislocation structure appearing in the material, both the X-ray diffraction (XRD) and the electron backscatter diffraction (EBSD) methods [16] were used. Such an analysis provides a possibility to give an adequate

* Corresponding author at: Mechanics and Physics of Solids Research Group, School of MACE, The University of Manchester, Manchester M13 9PL, UK.
E-mail address: elbor7@gmail.com (E.N. Borodin).

https://doi.org/10.1016/j.matchar.2018.05.002
Received 7 February 2018; Received in revised form 1 May 2018; Accepted 1 May 2018
Available online 04 May 2018
1044-5803/

estimation of scalar density of dislocations in the centre of a dislocation cell/grain (in the present work these dislocations will be referred to as mobile dislocations) as well as in boundaries (these dislocations will be referred to as immobile (or locked) dislocations). In some works (ex. [1]) an average size of a dislocation cell and an average size of a grain are measured independently. In these works, the received size of dislocation cell is always less as compared to the average size of a grain. Having a number of different measurable parameters of material microstructure evolving in the process of deformation, it is natural to raise a question about the role of each individual parameter for the dynamic recrystallization of material. The scheme presented in [17] makes it possible to describe all the main stages of dynamic recrystallization, but the mechanism of transformation of low angle boundaries of subgrains into high angle boundaries of grains remains unclear. A significant role of existing stress concentrators for this process is evident.

On the other hand, from mechanical point of view, two main issues arise in connection with SPD technologies: (i) a possibility to control all the above mentioned microstructural parameters by the process of plastic deformation and (ii) the degree of influence of each of the parameters on the resulting mechanical properties of the material. To date, the latter question is studied to a much better extent [3,9,13]. In order to understand microstructural processes, discover possibilities to control these processes and grasp the limitations imposed by these processes on maximum achievable material properties there is a need for development of new physical models of plastic deformation. These models should explicitly incorporate the above-mentioned parameters of microstructure as model variables. Plasticity models available to date [18,19] are not able to reflect neither the diversity of elements of microstructure evolving in the process of deformation nor the dynamical nature of different transient processes provided by varied process rates. In recent publications [20,21] the authors present 3D FEM simulation of SPD utilizing interesting rheological models. In [21] the authors observe an interesting regime of strain localization by formation of shear bands during ECAP. The most prominent models of dislocation plasticity widely used for simulation of different SPD processes [23–26] were proposed by Y. Estrin et al. [5]. A very peculiar modification of the model [5,6] has been recently proposed in [22]. The modification makes the model more accurate, taking into account strain rate dependence and correcting several imperfections in the initial system of equation. In a number of works the authors simulate evolution of dislocation density in a whole volume of a sample subjected to ECAP process (ex. [23]). Within the framework of these models, it is possible to receive realistic estimations of distributions of dislocation densities within the material as well as estimations of average grain size. Simulations utilizing these models provide significantly more information as compared to purely mechanical simulations using von Mises type limiting condition as a plasticity model [27–29]. Among disadvantages of the approaches originating from [5], one can mention a big number of fitting parameters that do not have a clear physical interpretation and no robust method of experimental evaluation. Another deficiency is a disability to predict evolution of the rest of the above-mentioned parameters of material microstructure.

Based on the approach presented in [30], the paper presents an attempt to establish consistent relationships between different processes associated with evolution of microstructure in metals subjected to SPD. It is particularly noteworthy that simulations utilizing the presented approach provide a possibility to predict scalar density of mobile and immobile dislocations, average size of dislocation cells, average grain size, grain aspect ratio, grain sizes, HAGBs fraction as well as the distribution of these parameters within the bulk of the processed material. The same model gives a possibility to account for the effect of strain hardening on the process of deformation.

2. Models Predicting the Evolution of Material Defect Substructure in the Process of SPD

2.1. Models of Dislocation Plasticity

Within the framework of classical model scalar dislocation density as a function of strain ε is given by [31,32]:ρ_D

$$\rho_D'(\varepsilon) = C + A\cdot\sqrt{\rho_D(\varepsilon)} - B\cdot\rho_D(\varepsilon), \tag{1}$$

where the first two terms $C\sim\delta_0\sigma_y{}^0/Gb^2$ and $A\sim\delta_f/b$ are responsible for dislocation density increase as a result of nucleation on dislocation forest and inclusions and the last term $B = k_\alpha$ stands for annihilation of dislocation pairs. Here G is the material shear modulus, b is the Burgers vector, $\sigma_y{}^0$ is the yielding limiting stress for dislocation free annealed material. Model parameters, δ_f and $k_\alpha$are, in essence, fitting parameters that should be evaluated empirically. For the case of $C = 0$ the equation is transformed into one of the variations of the classical "logistic" differential equation predicting the increase of population with the following saturation to limiting density given by: $\rho_D{}^{\max} = (\delta_f/k_\alpha d)^2$. A solution of the logistic equation has an exponential form with respect to deformation:

$$\rho_D = \rho_D^{\max}\left(1 + \left(\sqrt{\frac{\rho_D^{\max}}{\rho_D^0}} - 1\right)Exp[-B^2\varepsilon/A]\right)^2, \tag{2}$$

where $\rho_D{}^0$ is the initial dislocation density in the deformed material. In this case Eq. (1) can be rewritten as:

$$\frac{d\rho_D}{d\varepsilon} = \frac{\delta_0}{Gb^2}\sigma_y^0 + k_a\rho_D\left(\sqrt{\frac{\rho_D^{\max}}{\rho_D}}\right). \tag{3}$$

Obviously, the model can easily be enriched with additional sources and sinks of dislocations. For example, one can account for annihilation of dislocations at grain boundaries of fine-grained material [25,33]. The central problem here is connected to the evaluation of coefficients for this equation and their dependency on temperature and other state variables. For averaged description of processes within the dislocation subsystem, an energy-based approach can be used. In [32] it is considered that parameters for model Eq. (1) can be presented as $\delta_f = \alpha\eta Gb^3/\varepsilon_L$, $\delta_0 = \delta_f\alpha^{-1}$, where $\alpha\sim0.5$ is the Taylor constant [31,34], $\varepsilon_L = 8eV/b$ is the elastic energy of dislocation unit length [33,34], $\eta\sim0.1$ is the fraction of work of plastic deformation stored in the form of defects [32]. For small strains, by various estimates [35,36] this value should be around 10%. For higher strains the value of η is reduced by several times [36]. Using these parameters, it is possible to receive estimations for logistic equation type kinetic model parameters [32] $\delta_f\sim0.01$ and $\delta_0\sim0.02$. These values are normally utilized for simulations employing the classical model [31]. Dependencies of dislocation annihilation coefficients on temperature T and other state variables were received in a number of papers. Here one can mention the works of Galindo-Nava [37], where the annihilation coefficient is presented as:

$$k_\alpha = \left(\frac{G(T)}{G_0(T)}\right)^2\frac{1}{100b\alpha}. \tag{4}$$

Other equations for k_α were received by A. Vinogradov [38] and G.A. Malygin [31]. The definite form for (4) is given by $G(T)$, that, for different approximations, can have linear (or quadratic for k_α) dependency on temperature, as discussed in [39]. In [37] $G(T)$ is given as an exponential function of temperature:

$$G(T) = (4.74\cdot10^4)Exp[-3.97\cdot10^4T]. \tag{5}$$

In [37] k_α is approximated by:

$$k_\alpha = \frac{2+2\alpha}{1+2\alpha}\frac{b\nu_0}{\overline{V}_D}Exp\left[-\frac{\Delta G}{k_b T}\right], \tag{6}$$

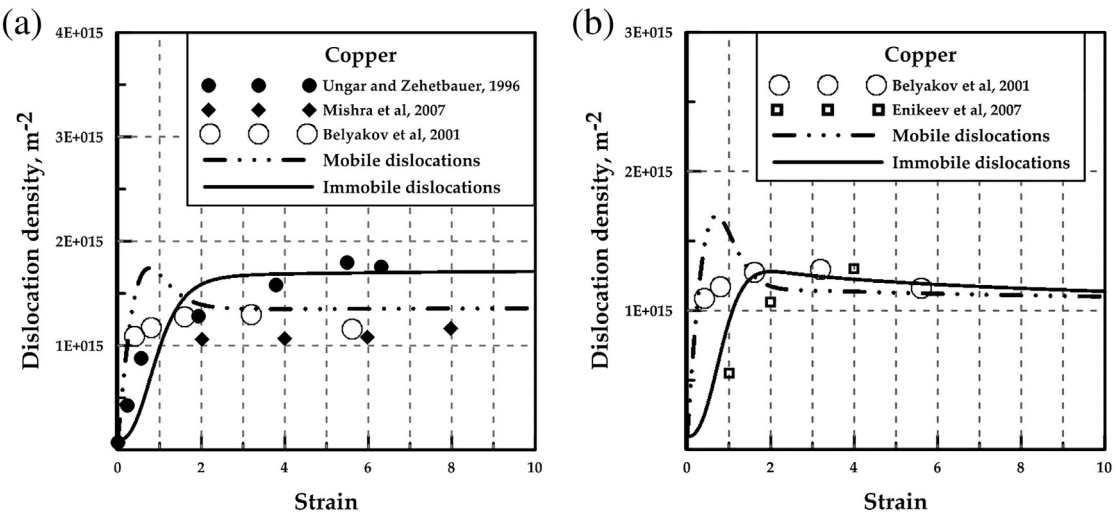

Fig. 1. The scalar density of mobile and immobile dislocations in the process of SPD as a function of accumulated strain. Points correspond to experimental measurements presented in [2,18,22,46].

where ΔG is the free Gibbs energy, $\overline{V_D}$ is the average dislocation velocity, k_b is the Boltzmann constant and ν_0 is the Debye frequency. Unlike previous papers, in [40] for aluminium k_α is given as a quadratic function of temperature. Another important parameter of the model is the static yielding limit of material σ_y^0. Material yield limit has the meaning of barrier stress that should be exceeded in order to initiate dislocation sliding. Its temperature dependency for copper can be presented as [37]:

$$\sigma_y(T) = 73.21 + (3.5\cdot10^{-3})T - (1.33\cdot10^{-5})T^2. \tag{7}$$

Obviously, for moderate temperatures the previous dependencies will not significantly affect the process of deformation of a copper sample. At the same time, for fine-grained materials, dependencies of yield limit on dislocation density and grain size are essential. The change of the yield stress in the process of deformation can be predicted using the Taylor law and the Hall–Petch empirical relationship [41]:

$$\sigma_y^0 = \sigma_D^0 + a_0 Gb\sqrt{\rho_D} + K_{\mathrm{HP}}/\sqrt{d}, \tag{8}$$

where $\sigma_D{}^0$ is conditional to the Peierls stress, impurities and all the other factors not connected with dislocations or grain boundaries. Here $a_0 = 0.4$ is the Taylor constant and $K_{\mathrm{HP}} = 0.1 \pm 0.06$ MPa $\mathrm{m}^{1/2}$ is the Hall–Petch constant for copper [42].

As discussed in [30] and confirmed by utilization of (1) in a number of succeeding papers [43,44], the approach based on Eqs. (1)–(7) is sufficient and "generally" suitable for modeling of intensive plastic deformation. At the same time Eq. (1), obviously, does not reflect many of the significant microstructural features of the process of plastic deformation. These non-reflected features do also have significant effect on mechanical deformation of the sample. First of all, this regards the arrest of moving dislocations and the formation of "dislocation forest" which, in other words, is the separation of dislocations into mobile and immobile dislocations (or, using different terminology, statically stored and geometrically necessary dislocations). With some variations, such a separation was performed in several models [4–6,34]. An approach presented in [4–6], and with modifications utilized in a big number of works [25,26,40,45,46] explicitly separates the material volume into two subdomains representing interiors of material dislocation cells and dislocation cell boundaries (the fraction of which increases with time as a consequence of localized dislocation arrest). Densities of dislocations existing in these two subdomains are treated separately. The key parameter for this model is the volume fraction of material representing grain boundaries. The thickness of cell boundaries and, consequently, the volume fraction of cell walls is assumed to be increasing with time. Coefficients of annihilation for dislocations localized in either of two subdomains are usually taken to be the same [4]. It should also be noted that this model predicts monotonous growth of mobile dislocation density, which is in contradiction to a number of available experimental data [1,2,25].

In [34] similarly to [5,6], it is supposed that the full dislocation density can be received as a sum of densities of mobile $\rho_D{}^{mob}$ and immobile $\rho_D{}^{im}$ dislocations. At the same time, in [5,6] it is supposed that cell (or mobile) and cell-wall (or immobile) dislocations are separated in space, occupying different fractions of volume, and these fractions can change in the process of deformation. Unlike [5,6], in [34] it is supposed that both dislocation types (mobile and immobile) are uniformly distributed within the same volume. This fact significantly simplifies the model. In [34] equations for high rates of deformation were proposed. In [32] authors reveal interconnection between energetic coefficients used to predict dislocation nucleation and coefficients of Eq. (1). For small rates of deformation, evolution of dislocation densities (taking into account the Orowan equation $\dot{\varepsilon}_{plast} = \rho_D^{mob} b\,|V_D|$ for plastic strain rate) is given by the following kinetic equations [30]:

$$\begin{aligned}\frac{d\rho_D^{mob}}{d\varepsilon} &= (k_g b\sigma_y^0 + \alpha Gb^2 k_g\sqrt{\rho_D^{im}+\rho_D^{mob}}) - \frac{V_C(\rho_D^{mob}-\rho_D^0)\sqrt{\rho_D^{im}}}{\dot{\varepsilon}_{pl}} \\ &\quad - k_\alpha^m(2\rho_D^{mob}+\rho_D^{im}) \\ \frac{d\rho_D^{im}}{d\varepsilon} &= \frac{V_C(\rho_D^{mob}-\rho_D^0)}{\dot{\varepsilon}_{pl}} - k_\alpha^i\rho_D^{im}\end{aligned} \tag{9}$$

Here $k_g = \eta/\varepsilon_L b$ is the coefficient responsible for dislocation generation [32,33]. Here, similarly to [5,6] the second component (immobile dislocations) is formed by "settling" of the dislocations of the first group (mobile dislocations), which are initiated at obstacles following one of the possible nucleation mechanisms. Unlike model [5,6], in [34] for the second component (immobile dislocations) there is no generation of new dislocations due to existing immobile dislocations. This is the result of the fact that these dislocations are "immobile" (i.e. not moving) and generation of new dislocations following any of the known mechanisms requires motion of existing dislocations. It can be noted that overwhelming majority of these dislocations should be located in a vicinity of grain boundaries or within dislocation forest.

The received dependencies (see Fig. 1a) are compared to results of several different experimental measurements [2,18,25,48]. For the used values of model parameters (first of all, the immobilization rate) the two dislocation densities are not substantially different. It is remarkable that the mobile dislocation density has a marked maximum for the

values of deformation close to 1. This stage of deformation correlates with the stage of active comminution of material sub-grain structure (e.g. see Fig. 5) when the fine-grained structure is yet not fully formed and an active generation of new dislocations within grains is ongoing. Such a maximum was observed experimentally for copper subjected to HPT in [47].

Besides the maximum discussed above, in experiments [2,25,47] another local maximum of dislocation density is observed for accumulated strain equal to 2–4. This maximum can be explained not by a formation of dislocation structure, but by a formation of grain structure within the deformed material. It is necessary to account for an additional sink of dislocations into grain boundaries and decrease of dislocation density due to transformation of cell walls into grain boundaries. The influence of these processes is of a special importance for deformations in the range between 1 and 3 when intensive dynamic recrystallization is taking place and multiple cells are transforming into grains. Additional sink for mobile dislocations, accounting for this process can be included into Eq. (9) similarly to [49], where it was employed for description of fine-grained materials:

$$\rho_D^{(-)} = \rho_D V_D / d. \tag{10}$$

Subtracting $\rho_D{}^{(-)}$ given by Eq. (10) from the first of Eq. (9) will account for the additional dislocation sink. Obviously, the magnitude of this term will strongly depend on the material grain size.

Fig.1b shows the results of modeling while accounting for that additional dislocation sink. Accounting for dislocation sink at grain boundaries leads to a possibility of dynamic equilibrium between dislocations generated within grains and their annihilation at grain boundaries for large strains (Fig. 1b) (and resulting decrease of average grain size compared to Fig.1a). In [25] a similar dislocation drain is introduced, describing the dissolution of dislocations in grain boundaries for materials subjected to ECAP process. An additional term accounts a probability of this dissolution (about 30% as estimated by the authors). Such a modification gives a possibility to enrich the utilized plasticity model [5,6] and achieve a correct prediction of existing experimental curves.

It should be noted here that a comparison of theory to experimental observations is not a trivial question since the quantities measured in experiments using electron microscopy or X-ray structural analysis only partially correspond to the variables used in numerical simulations. Thus, the density of dislocations registered at the grain interiors should only nominally correspond to the density of mobile dislocations. At the same time, these two values follow similar kinetic laws and therefore should have at least the same order of magnitude. Explicit separation of the total density of dislocations into density of mobile and immobile dislocations gives a possibility for a natural account of the dynamic, non-equilibrium nature of the evolution of material defect substructure in the process of deformation. In particular, this provides a possibility to propose a model of dynamic recrystallization, explicitly taking into account the degree of deviation of the system state from equilibrium.

2.2. Size of Dislocation Cells

It was shown experimentally that a whole set of various dislocation substructures can be implemented within plastically deformed material. In some cases, these substructures may succeed each other at different stages of plastic deformation [50]. Wherein, for the late stages of deformation, corresponding to severe plastic deformation, it is customary to consider dislocation cell as the basic structure observable in the material at the mesoscale level [1]. The size of dislocation cells can be estimated from energetic reasoning [51]. If one compares energy of a group of dislocations homogeneously distributed in a unity of volume and the energy of dislocations (per unit volume) within the walls of dislocation cells [52], it will be found that above some definite dislocation density, it is energetically favourable to form dislocation cells, rather than maintain homogeneous distribution of dislocations. Searching for equality of energies of homogeneous distribution and the cell dislocation structure, critical dislocation density leading to cell formation can be found [51] $\rho_D{}^* = (3e/8d)^2$, here e~2.71. Thus, dislocation cell diameter as a function of dislocation density can be received as:

$$D = \beta \rho_D^{-1/2}. \tag{11}$$

Here β is a coefficient of the order of 1 that is dependent on dislocation cell geometry. Obviously, so far, the scalar density of dislocations has a meaning of full length of dislocation lines per unit volume (having a dimension of m^{-2} or cm^{-2}), Eq. (4) with $\beta = 1$ is valid to predict distance between dislocations assuming uniform spatial distribution of dislocations in the material volume. It can be shown [51], that for elliptical cells β~1, for spherical cells $\beta = 2.6$. At the same time, this dependency does not give a possibility to establish interconnection between the size of a dislocation cell and the size of grain structure formed within the material in the process of deformation. Experimentally observed sizes of both the grains and the cells appear to be an order of magnitude larger as compared to values predicted by (11) with β~1. In order to describe the dynamic recrystallization curve, β should attain values of at least 20–30 [4,6] and be reduced by the factor of 4–5 with the reduction of grain size from tens of micrometres to hundreds of nanometres [53]. This fact makes Eq. (11) practically inapplicable for prediction of dynamic recrystallization. At the same time, this equation apparently can give an adequate description for evolution of dislocation cell network.

In [37] an equation for calculation of coefficient β from (11) including its temperature dependence was proposed:

$$\beta = \frac{24\pi(1-\nu)}{(2+\nu)}\left(\frac{1}{2} + \frac{T\Delta S}{Gb^3}\right), \tag{12}$$

where $\Delta S = k_B Ln\left(\frac{\dot{\varepsilon}_0 + \nu_l}{\dot{\varepsilon}}\right)$ is the statistical entropy [54], $\nu_l = \nu_D Exp(-E_m/RT)$ is the vacancy migration frequency with ν_D~$10^{13} s^{-1}$ being the Debye frequency, R being the gas constant and $E_m = 87 kJ/mol$ being the vacancy migration energy, $\dot{\varepsilon}$ is the deformation rate of the material, $\dot{\varepsilon}_0 = bc_s\rho_Y$ is related to the sound velocity $c_s = 3810 m/s$ and ρ_Y is the dislocation density consistent with the yield point [55]. For typical parameter values this expression yields β~11.

Understanding the transformation of dislocation cell walls (having significant widths and low angles of misorientation between neighboring cells) into grain boundaries (with widths of the order of nanometer and misorientation angles exceeding limiting value achievable for any dislocation structure) is one of the important unsolved fundamental problems of contemporary material science. Dynamic recrystallization in the process of severe plastic deformation has been studied by several authors [1,17]. It is obvious that at some point of time a local transformation of dislocation cells into a low-angle grain boundary takes place. It can be assumed that this process is determined by non-equilibrium state of cell boundaries affected by intensive annihilation of dislocations pairs (due to their migration) and immobilization of the new lattice dislocations. Experimental observations [17] testify the significant influence of these processes on dynamic recrystallization. Besides that, another important factor affecting dynamic recrystallization is the effect of stress concentration at cell boundary triple junctions (TJs). Taking into account both of these factors it is possible to propose a non-equilibrium model of dynamic recrystallization, having the fraction of non-equilibrium grain boundaries and the state of grain boundary triple junctions as the main model variables.

2.3. Non-equilibrium Model of Dynamic Recrystallization

Experimental studies of dynamic recrystallization of various materials are presented in a sufficiently large number of works [10,17,18,47,56] including a number of reviews [1,9,12,13] on the

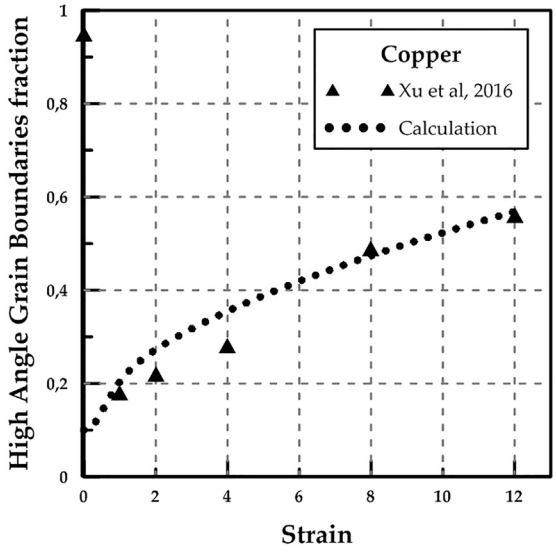

Fig. 2. Fraction of nonequilibrium grain boundaries as a function of accumulated strain [61].

topic. The development of experimental methods, in particular HR (High Resolution) TEM-microscopy makes it possible to investigate the evolution of the microstructure of metals at different stages of plastic deformation in every detail. Traditionally, materials subjected to SPD display lognormal distribution of grain sizes [7,57]. Often the distribution is bimodal and large submicron grains coexist with nanosized grains [56,58]. A wide range of defect structures can be observed in metallic materials: dislocation-free grains, non-equilibrium grain boundaries, dislocation cells and subgrains, low- and high- angle grain boundaries, stacking faults and micro-twins. Differently sized grains have diverse properties and may have a varied impact on further recrystallization of the material. For example, grains sized about 1 mm are often split into 4 subgrains with diameter of several hundred micrometres. A theoretical model for this mechanism employing disclination methodology was presented in [59]. The succeeding deformation results in increase of angles of misorientation between subgrains to high angle boundaries ($\theta > 15^{\circ}$) [1]. Another possible mechanism that can result in appearance of significant fraction of large-angle grain boundaries is the development of localized microscopic shear banding with LAGB structure formed between microscopic shear bands [60]. Sub-micron sized grains with sizes larger than 200 nm contain higher density of intergranular dislocations and are more deformed as comparing to nanocrystalline grains. They are also significantly elongated along the main direction of deformation and have large aspect ratio. Dislocations that are randomly distributed within these grains form the structure of the low-angle subgrains appearing in the process of subsequent deformation. Inside grains with sizes within sub-micron range (100 nm–1 μm) one can often find subgrain structures of substantially (up to an order of magnitude) smaller sizes with some of the boundaries being LAGBs and some of them being HAGBs. Non-equilibrium grain boundaries are often found for grains sized 100 nm–500 nm. Intensive elastic stress fields are observed in a vicinity of these boundaries. According to [61] such high-energy grains, possessing long-range stress field, can be formed by absorption of a large number of lattice dislocations. In [17] it was noted that large grains have noticeably curved boundaries with a large number of grain boundary dislocations. Local concentrations of dislocations in the grain boundaries and grain boundary TJs (triple junctions) for such grains can be 2–3 orders of magnitude greater than the average ($3 \cdot 10^{13} - 5 \cdot 10^{14} m^{-2}$) [10] and measure up to $2.5 \cdot 10^{17} m^{-2}$ [17]. Remarkable is the role of stacking faults caused by splitting of lattice dislocations and micro-twins. This process should also contribute to the formation of the grain structure. Nanometer-sized grains apparently grow from nuclei adjacent to stress concentrators at later stages of the deformation process [17]. The above data corroborate the complexity and multistage nature of dynamic recrystallization process at which an essential role should be devoted to grain boundary TJs and flows of lattice dislocations annihilating near grain boundaries and inside dislocation cells. Dislocation plasticity model, by itself, does not provide an exhaustive description of these processes and therefore should be enriched by additional information accounting for the role of non-equilibrium boundaries and TJs being the important factors of dynamic recrystallization.

Consider the formation of non-equilibrium high-angle grain boundaries (HAGBs) to be the main factor controlling dynamic recrystallization of material. In order to do so, the fraction of high angle grain boundaries, a parameter that is measured experimentally as a part of EBSD analysis can be employed. As mentioned earlier, this type of boundaries cannot be formed as a result of evolution of dislocation boundaries. Apparently, the increase of misorientation angle across the boundary (i.e. transformation of LAGB into HAGB) requires a non-equilibrium state when a dislocation boundary is being "bombarded" by lattice dislocations accompanied with their active annihilation. Another important factor is the presence of disclination-type stress concentrators [62] in cell boundary TJs. From experiments (for ex. with copper [2]) it is known that fraction of HAGBs for moderate strains (usually between 2 and 6 [1,2]) is a quasi-linear function of the accumulated strain. The key point for the present consideration of dynamic recrystallization is the dependence of the LAGBs fraction on the processes of dislocation kinetics and the state of the material microstructure at each instant of time. Within the framework of this conception of nonequilibrium nature of transformation of LAGBs into HAGBs under the influence of the process of immobilization of dislocations at the boundary and the process of dislocation annihilation, the rate of nonequilibrium grain boundaries fraction change should be proportional to the ratio of mobile to immobile dislocations V_C [34]:

$$\rho_D^{V_C^{(-)}} = V_C(\rho_D^{mob} - \rho_D^0)\sqrt{\rho_D^{im}}. \tag{13}$$

In this case, the growth rate of HAGBs/nonequilibrium boundaries fraction p can be presented as:

$$\dot{p} = \chi \rho_D^{V_C^{(-)}} d/D. \tag{14}$$

Here χ is an empirical parameter. Fig. 2 presents a comparison of calculations using Eqs. (9), (11) and (14) with parameters listed in Table 1 to experimental measurements [2,18,63]. In order to estimate grain sizes, equations of dynamic recrystallization were used. These equations will be presented below. The large deviation between the first experimental point in Fig. 2 and the calculated curve is due to the initial state of material for which the fraction of HAGBs is high. Already after the first SPD pass this fraction is reduced by a factor of 5 due to

Table 1
Model parameters for copper evaluated from correspondence to experimental data [2,18,61].

Model parameters	V_C	k_a	k_g	χ	Taylor constant	β
Values	$5.8 * 10^{-8}$	1.9	$5.8 * 10^{16}$	12.7	0.4	11
Material parameters	Shear modulus, GPa	Burgers vector, nm	Temperature, K	Static yield stress, MPa	Initial dislocation density, m^{-2}	Initial grain size, μm
Values	46	0.256	300	130	10^{14}	1

formation of lower scale structure with low angle cell boundaries. The following quasi-linear growth with saturation is accurately modelled by the Eq. (14). Immobilization rate for lattice dislocations determined by V_C and the flow of cell dislocations onto the boundary determined by ρ_D^{mob} control this process. Obviously, in order to estimate the sizes of material cells and grains, the Eqs. (9) and (14) should be consistent between each other and with the subsequent equations of dynamic recrystallization.

For sufficiently uniform distribution of grain orientations histogram [60], it is possible to introduce the average misorientation angle, as done by several authors [1,2,54]. Undoubtedly, for bimodal or substantially nonuniform distribution of the grain orientations the utilization of this parameter is incorrect and no longer reflects the actual material characteristics. However, it is extensively used by many authors. An empirical expression for the average angle of misorientation between neighbouring grains is given in [54] and has the form:

$$\bar{\theta} = k_\theta \varepsilon_{pl}^{2/3}, \tag{15}$$

where the proportionality coefficient k_θ can be received as $k_\theta = (3/2)^{1/3}(4T\Delta S/\beta G b^3 M)^{2/3}$ with $M \sim 3$ taken from the Taylors equation $\varepsilon_{pl} = M\varepsilon$ [64]. The equation for the angle of misorientation between neighbouring grains was proposed in [25] based on dislocation concepts. According to [25] the rate of the angle change is proportional to the probability of immobilization of a lattice dislocation by the grain boundary (1/3), is proportional to the local dislocation density and is inversely proportional to the size of the grain. Within the framework of the developed theory it is natural to assume that the average angle of misorientation is proportional to the fraction of HAGBs, since they are the major contributors to this angle. In this case:

$$\bar{\theta} = sp. \tag{16}$$

where s defines an average value of misorientation angle typical for material HAGBs and p gives the fraction of these boundaries. Fig. 3 gives the average misorientation angle as a function of accumulated strain calculated using Eqs. (9), (11), (14) and (16). The dependency received for $s = 15^\circ$, being the avowed value of misorientation angle for which the grain boundary is considered to be a HAGB, coincides with the experimental points [54] and the predictions received using Eq. (15). In order to receive coincidence with experiments presented in [2] the value of $s = 55^\circ$ is required (see Fig. 3), which is apparently due to a more complex function of misorientation angle distribution.

Consider the state of grain boundary TJs and their evolution in the process of deformation. Experimental measurements [65] yield dependencies for fraction of triple junctions with 0,1, 2 or 3 adjacent HAGBs, denoted as J_0, J_1, J_2, J_3 accordingly. As the first approximation, these dependencies can be received as [65]:

$$\begin{aligned} J_0 &= (1-p)^3 \\ J_1 &= 3p(1-p)^2 \\ J_2 &= 3p^2(1-p) \\ J_3 &= p^3 \end{aligned} \tag{17}$$

Fig. 4a shows the corresponding dependencies as a function of accumulated strain computed using Eqs. (17), (9), (11) and (14). Another model presented in [65] provides a more accurate description of experimental data measuring the number of TJs with a different number of adjacent HAGBs, but the corresponding equations appear to be much more complex. Fig. 4b displays calculations using the refined model. The corrections are mainly important for strain dependency of the fraction of TJs with one and two adjacent HAGBs (J_1 and J_2). Being a part of the presented below model of dynamic recrystallization, this correction does not significantly affect (resulting effect is in the range of few percent) the dynamic recrystallization curve. Factions of triple junctions with 2 and 3 nonequilibrium grain boundaries increase slowly even for a large number of SPD passes and do not exceed 20–30%. At the same time, according to the refined model, the fraction of grain boundary TJs with a single nonequilibrium boundary quickly reaches saturation at around 60%.

Here it is assumed that the main event affecting the process of dynamic recrystallization is not the formation of separate dislocation boundaries, but the formation of stable triple junctions of these boundaries or, in other words, the formation of static points for the future grain structure. These static points serve as stress concentrators, affecting the flow of dislocations onto the grain boundary. It can be assumed, that strongly nonequilibrium state of dislocation cells boundaries, resulting from an intense flow of inner cell dislocations and their intensive annihilation, leads to an increase of the power of disclinations inside TJs, arrest of TJs migration [66] and the formation of disclination-type defects with stress fields that eventually lead to transformation of dislocation cell walls into grain boundaries. Similar processes of formation of dislocation walls between disclination-type stress concentrators with subsequent separation and migration of partial disclinations at different configurations were simulated in [62]. Therefore, here it is assumed that the average size of the emerging grain structure is the same as the distance between adjacent triple junctions. It is also supposed that the cell structure is continuously evolving in compliance with “equilibrium” Eq. (11). The evolution of dislocation cell structure does not reflect the evolution of grain structure and these processes can coexist. Should it be supposed that during this process a part of the elements of the future grain structure is consequently consolidated with time, then every definite level of plastic strain corresponds to a definite size scale, larger than the size of dislocation cells. The size is given by Eq. (11). This size corresponds to the mean distance between consolidated elements (immobile triple junctions) of the future grain structure. If a volume fraction of consolidated triple junctions $J = J_1 + J_2 + J_3$ is introduced, then the mean distance between the elements of stable structure will be given by:

$$d = \frac{\beta}{J}\rho_D^{-1/2} \tag{18}$$

Fig. 5 gives dependencies of the average size of dislocation cell (calculated according to (11)), the average size of grain (calculated according to Eq. (18) with $J = J_1 + J_2 + J_3$) and the average size of grain surrounded by HAGBs (calculated according to Eq. (18) with $J = p$) for SPD processed copper. Least time is needed for evolution of dislocation cells. According to Fig. 5, average dislocation cell diameter is reduced by several times already for strain ~1. The Eq. (18) together with the Eqs. (9), (11) and (14) demonstrate a delay of recrystallization

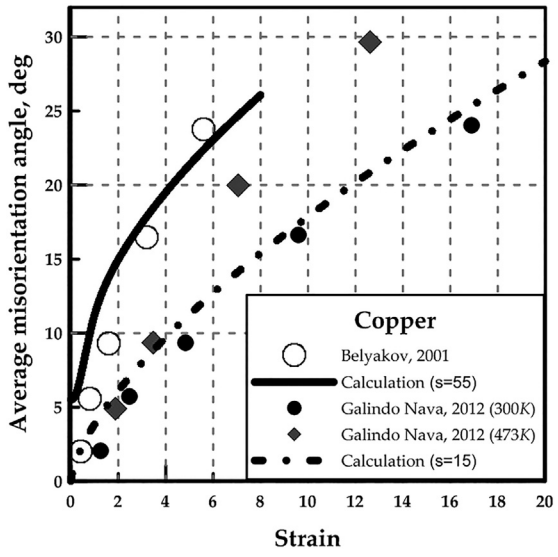

Fig. 3. Average angle of grain misorientation as a function of accumulated strain [2,34].

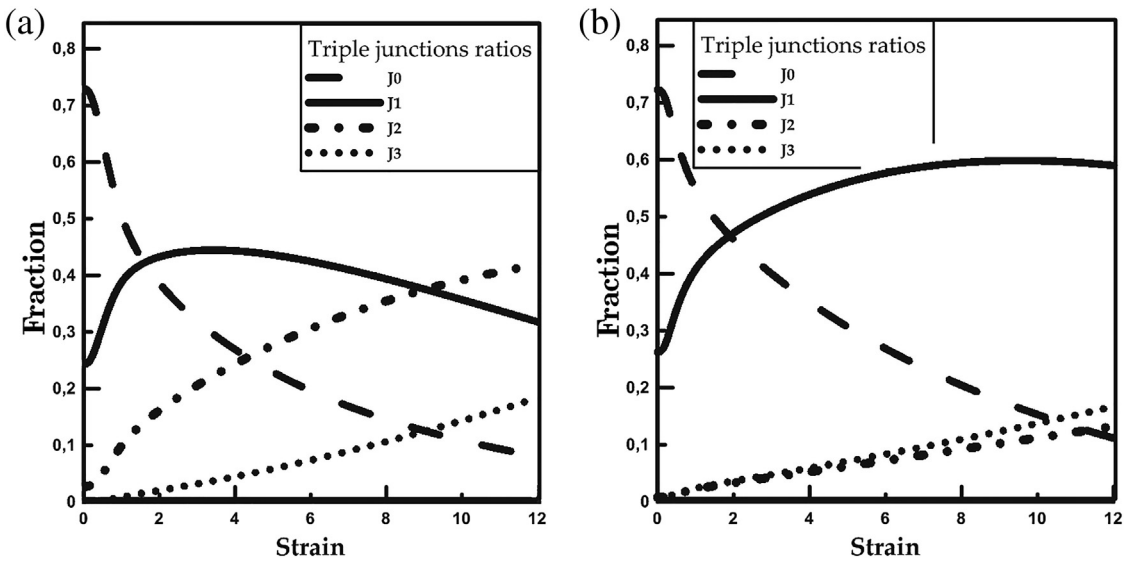

Fig. 4. Fraction of grain boundary triple junctions with 0,1,2 and 3 HAGBs calculated using the simplified (a) and the refined [63] (b) model.

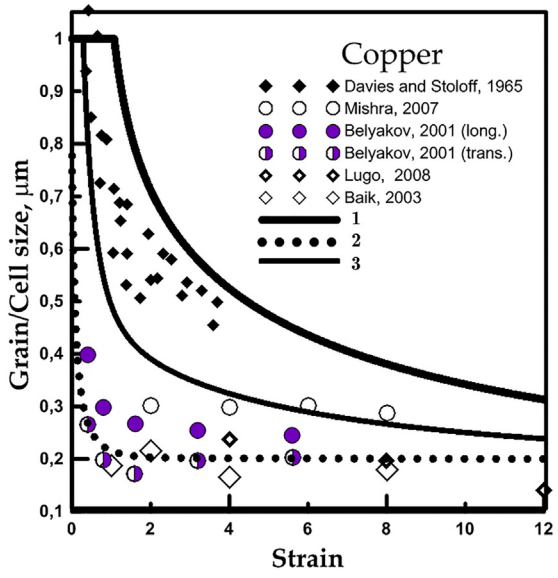

Fig. 5. Dynamic recrystallization in copper. Comparison of experimentally measured sizes of microstructure (scattered points) to theoretical predictions (lines 1, 2, and 3) for different values of accumulated strain. 1 is giving the average size of grain surrounded by HAGBs (misorientation angles exceeding 15°), calculated according to (18) with $J = p$. 2 is giving the average size of dislocation cell (calculated according to (11) and 3 is plotting the average size of grain (calculated according to (18) with $J = J_1 + J_2 + J_3$).

up to the strains ~1 for grain boundaries and up to the strains ~2 for high-angle grain boundaries, which is in a good coincidence with known microstructural studies [17]. Experimentally measured dimensions of grains and cells as a function of accumulated strain for copper are characterized by significant scatter and, in many cases, it is difficult to understand what kind of structures are actually measured by the corresponding microstructural analysis. Qualitatively, the developed theory is in a good coincidence with experimentally observed dependencies and provides a correct estimation of dissimilarity between the average size of a grain and the average size of a dislocation cell that usually appears to be several times smaller.

Another microstructural characteristic that can be measured experimentally is the grain aspect ratio $E = \varepsilon_{\parallel}/\varepsilon_{\perp}$, with $\varepsilon_{\perp}$ being the minimum grain dimension (measured in the cut plane) and $\varepsilon_{\parallel}$ being the maximum grain dimension. For a homogeneous deformation without recrystallization this value is given by $(1 + \varepsilon)$. In experiments [2] the difference between the longitudinal and the transverse dimension can reach 20%–50%, accordingly $E = \varepsilon_{\parallel}/\varepsilon_{\perp} \sim 1.2 - 1.5$. The value of E reaches its maximum for strains in the range between 1 and 3. For higher strains E is approaching 1. For considerations of dynamic recrystallization, the importance of grain aspect ratio consists in peculiarities of dynamic recrystallization process that are apparently related to the evolution of the dislocation structure. According to rotational model of dynamic recrystallization [18] quasi-spherically shaped grains are formed in coarse-grain material. Subsequent deformation results in a significant deformation of initial grains in the direction of maximum elongation of the material. New dislocation walls are formed inside elongated grains. These dislocation walls can be later transformed into new grain boundaries resulting in reduction of the grain size and the aspect ratio E. For strain exceeding 3 the aspect ratio is close to constant.

2.4. Choice of Model Parameters and their Influence on Dynamic Recrystallization

The proposed model is a closed and self-consistent in the sense that it is completely determined by scalar densities of mobile and immobile dislocations, fraction of non-equilibrium grain boundaries and the size of dislocation cells and grains. Furthermore, all of these variables are interrelated between each other, so that a change in kinetic behaviour of one of them immediately impacts all the others. For such a number of variables, the model contains only a few parameters, most of which have clear physical meaning, theoretical estimations and are well researched. These model parameters are summarized in Table 1 along with parameters of the material evaluated for the initial state of the material microstructure. Central parameters affecting all of the model variables are the constant giving the generation of dislocations, the coefficient of annihilation, the rate of immobilization of dislocations and the coefficient of proportionality χ from the Eq. (14). All these parameters can be received from the analysis of experimental data giving dependences of dislocation density and fraction of HAGBs as a function of the accumulated strain. The most interesting outcome of the proposed models is the possibility to predict the dependence of the dynamic recrystallization on the annihilation rate and the dislocation immobilization rate. In practice these parameters can be controlled by additional introduction of impurities and other defects into the deformed material. Fig. 6 gives accumulated strain dependency for the

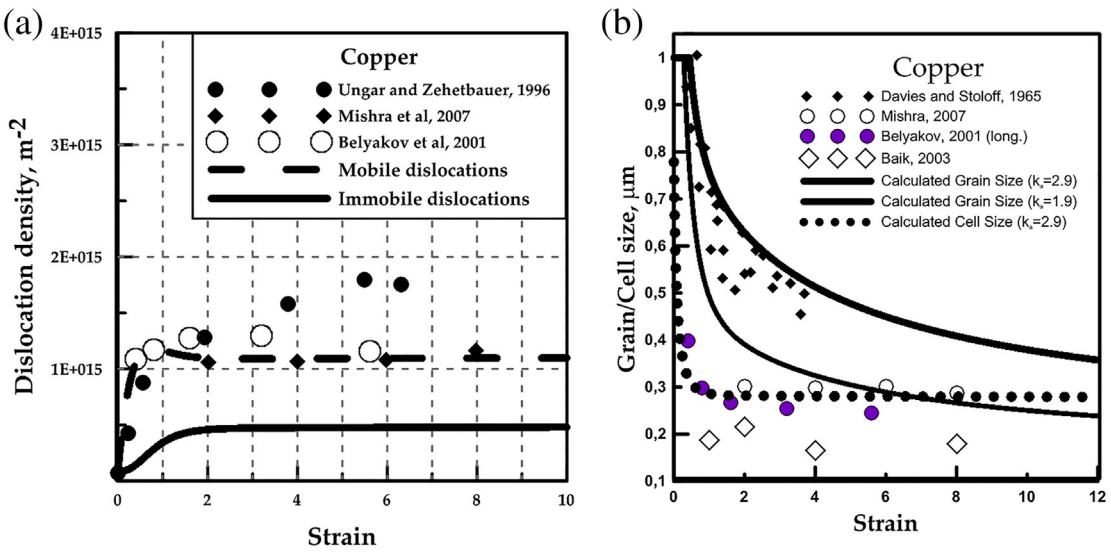

Fig. 6. Alternation of the all main dependencies for the increased value of dislocation annihilation parameter).

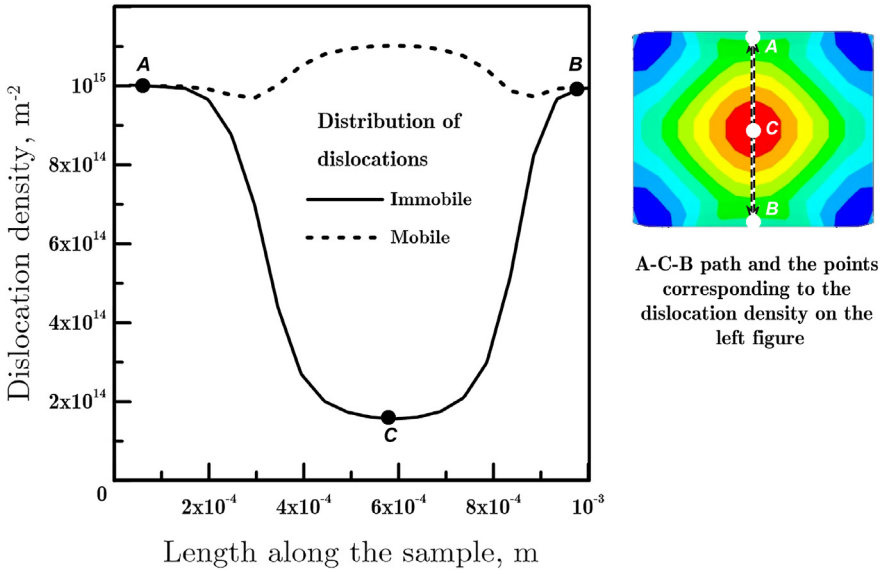

Fig. 7. Distribution of dislocation densities within the cross section of the sample after the first pass of multi-directional forging (MDF).

main model variables at the increasing value of parameter controlling annihilation $k_\alpha \sim 4$ (that results in the same effect as immobilization rate V_C). For comparison, experimental points discussed previously (Fig. 1, Fig. 5) are included in the Fig. 6.

3. Full three-Dimensional Modeling of Multidirectional Forging Utilizing the Developed Model of Microstructure Evolution Embedded into FEM Computational Scheme

The developed model was embedded into a computational code based on Finite Element Method (FEM). New plasticity models were implemented as USERMAT FORTRAN subroutine for ANSYS commercial finite element software. The subroutine is executed during element results calculation and provides a possibility to update local dislocation densities as well as the other microstructure-related parameters in every point of the deformed sample. The parameters controlling microstructure evolution are updated every integration substep according to the local material deformed state in compliance with the corresponding Eqs. (8)–(11), (14), (17) and (18). Conditions corresponding to those realized in experiments [2] are modelled. In these experiments copper samples initially shaped as parallelepipeds with dimensions of 9.8 mm by 8.0 mm by 6.5 mm are subjected to multidirectional forging. Experimental geometry is such that the ratio of the sample dimensions is the same after each deformation pass. Experiments were performed at room temperature at a strain rate approximately equal to $10^{-3}\,s^{-1}$. In the present study only the first pass of multiaxial forging is modelled. In [67] the authors come to a conclusion that for less than eight independent slip systems, only scalar flow rules need to be solved. This provides a possibility to assume symmetric distortion tensor for 3D calculations of deformation of copper alloys.

Since the process can be considered as quasi-static, time integration is not performed. The problem is formulated as a number of consequent static substeps given by displacement gradually applied to the moving part of the multidirectional forging die. Time is eliminated from the state equations. Stresses and strains in the deformed specimen on each substep are calculated according to elastic deformation model. Once a stress at some point of the bar reaches the value outside von Mises plastic flow surface, the plastic flow is onset at this point. The strain that appeared at that point due to displacement applied at the top of the sample is split into elastic and plastic parts, returning the stress to the

plastic flow surface. Alteration of plastic part of strain tensor is affecting dislocation densities Eq. (9) as well as the rest of the described material microstructure parameters according to Eqs. (8), (11), (14) and (18). Material properties are taken from Table 1.

Fig. 7 presents the results of modeling for distribution of dislocation densities within the cross section of the sample after the first pass of MDF. These dislocation densities were calculated according to Eq. (9) and therefore the number of immobile "forest dislocations" essentially depends on the utilized model parameters. For different experimental conditions, inducing different types of local deformations, the density of "forest dislocations" in the centre of the sample can both decrease or significantly increase after the first MDF pass. The model parameters used for this simulation were chosen based on coincidence to experimental data as discussed in the previous sections.

For the model presented in this paper, according to Eq. (8), the dislocation density (and dependent processes of dynamic recrystallization) determines the material strain hardening and, by this, affects the mechanical properties of the material. For the first MDF pass, as evident from Fig. 5 and experimental data [17], the material grain size does not change significantly. At the same time, dislocation density increases by an order of magnitude and dislocation cell size decreases by several times. Nonuniform distribution of dislocation density within the bulk of the material corresponds to nonuniformity of deformation of the sample in the mold. Fig. 8 presents computed heterogeneous distribution of strain within a sample after a single pass of MDF. It is noticeable, that in a sufficiently large zone located in the centre of the sample, strains can reach values close to 1. Simple geometric estimations for homogeneous distribution of strains [2] yield the value of 0.4, being 2–3 times less as compared to the actual strains. At the same time, it is the latter value of 0.4 that is usually used for plotting experimental dependencies for various material parameters on accumulated strain in the process of MDF.

Few papers are known, mentioning inhomogeneity in distribution of strains/microhardness throughout the volume of a sample after MDF. Among them the work presenting experiments with 2A14 aluminum alloy [68] which reported four different deformation zones in the sample. This effect is in a good coincidence with the simulation results received in this work. The corners of the mold are the most problematic regions for MDF deformation method. Due to this, pressing usually cannot be brought to the end of the cycle neither in calculations nor in experiments. Moreover, mold corners serve as stress concentrators significantly distorting the deformation pattern of the sample.

Influence of friction on interfaces between the sample and the mold has also been studied. Friction has been modelled as standard Coulomb friction with values 0.1–0.4 for friction parameters taken from [69] for the case of dry friction between the sample and the mold and the case of lubricated friction provided by various possible lubricants. No significant effect of friction on the received strain distribution has been observed for any of the utilized friction parameters. Neither in [69], where nonstructural approaches were used to model ECAP of copper, authors observed no significant influence of friction on simulation results.

Grain aspect ratio can be registered experimentally [2] (see experimental points Belyakov et al. at Fig. 5) and is determined by inhomogeneity of deformation along different directions. As observed experimentally, after the first MDF pass typical minimum and maximum grain dimensions of a grain differ by a factor of 1.5. Simulation gives a rather complex picture for distribution of principal stresses (in GPa) within the bulk of the sample (Fig. 9).

As follows from the presented figures, the magnitudes of the first (largest) and the third (smallest) principal stresses in the central region differ by the factor of 3. As shown in Fig. 8, the order of magnitude of the average dislocation density for 3D simulations coincides with the one-dimensional computations (see Fig. 5). This provides ground to state that the "one-dimensional" modeling of SPD processes presented in the foregoing sections is, in outline, correctly predicting the

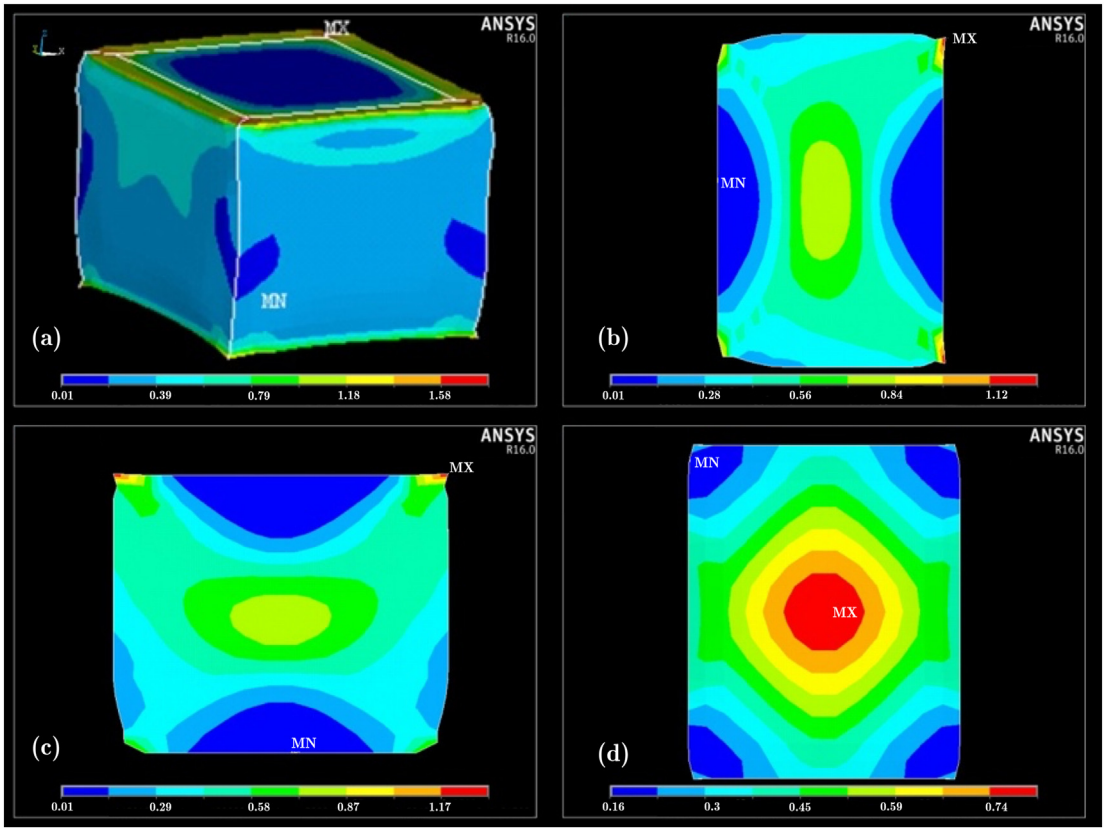

Fig. 8. Heterogeneous distribution of strain within a sample after a single pass of MDF.

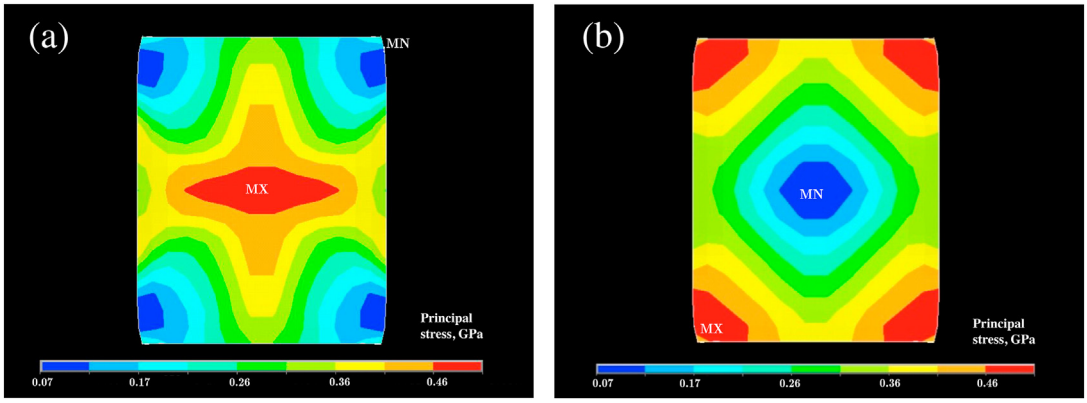

Fig. 9. Distribution of the largest (a) and the smallest (b) principle stress in gigapascals (GPa) after the first MDF pass.

evolution of the microstructure and mechanical properties of metals in the process of deformation. A similar result was received in [30] for ECAP simulations. At the same time, many significant features of material deformation are related to inhomogeneous distribution of strain within the bulk of the sample, and this should be taken into account while describing real SPD experiments. Thus, in [70,71] a gradient theory of dislocation plasticity is developed. This approach gives a possibility to take into account the additional contribution of the inhomogeneous distribution of dislocation density within the bulk of the material. For processes such as HPT [71], this becomes critical for simulations of experimental results. The main physical effects accounted by the approach [71] are the occurrence of geometrically necessary dislocations compensating for strain nonuniformity and the emergence of reaction stresses between adjacent grains of polycrystal due to plastic strain incompatibility.

4. Conclusions and Discussion

Detailed experimental microstructural studies of materials processed using different SPD techniques [1,2] provide a unique possibility to perform accurate comparison between these experimental measurements and predictions received utilizing the developed theoretical model. Dynamic recrystallization model proposed in this work is based on evolution of fraction of high-angle grain boundaries (HAGBs) and the associated fraction of grain boundary triple junctions with different number (between 0 and 3) of adjacent HAGBs. The process of the transformation of dislocation cell boundaries (characterized by relatively large widths and creating small misorientation angles across the boundary) into grain boundaries (characterized by much smaller thicknesses and creating large misorientation angles across the boundary) is supposed to be critical (and driving) for the entire process of dynamic recrystallization. Immobilization rate for lattice (mobile) dislocations, defined by the flow of mobile dislocations onto the cell boundary, can be used as a parameter decisive for the rate of transformation of cell boundaries into grain boundaries. In fact, this parameter is reflecting the degree of boundary “nonequilibrium” being the main factor of grain evolution. At the same time, it is supposed that the evolution of dislocation cells can be described by a usual approach – their size is back proportional to the square root of the scalar density of dislocations. In this way the models of dislocation density kinetics are forming a unified and consistent system of equations including expressions for the fraction of nonequilibrium boundaries, the size of dislocation cells and the grain size. In turn, the latter affects dislocation kinetics by the influence on the material yielding stress. This influence is accounted according to the Taylor law (for cells) and the Hall-Petch relation (for grain boundaries).

This new model significantly widens the range of possible applications for the previous models [5,6,34]. Furthermore, the new model stimulates new experimental investigations of grain triple junctions and topological changes of the grains structure during SPD. The most interesting feature of the developed model is the explicit dependency of all of the microstructure evolution processes on rate-dependent parameters such as the immobilization rate of mobile dislocations or the coefficient of their annihilation. In practice, these parameters can be controlled by changing the internal material microstructure, which opens wide perspectives for development of new SPD processes for production of new materials with unique mechanical properties.

It is remarkable that providing reliable predictions for a wide range of microstructural properties (HAGBs fraction, dislocation cell size, grain size, dislocation density in interior of a cell, dislocation density in a grain boundary, fractions of triple junctions with different number of adjacent HAGBs, grain aspect ratio), the developed model is utilizing a limited number of parameters having a clear physical interpretation and the corresponding physical models for parameter evaluation. Numerical simulations presented in this work are testifying the applicability and accuracy of the developed approach. For multi-directional forging of copper considered in this paper a fraction of non-equilibrium grain boundaries was calculated to be around 0.6. Also, a minimum dislocation cell size (200 nm), a minimum grain size (around 250 nm–300 nm), and a scalar dislocation density (around $10^{15}\,m^{-2}$) were estimated. Obviously, evolution of these parameters is greatly influenced by the utilized model parameters (such as the coefficient of annihilation for dislocation pairs or the rate of dislocation immobilization). The new abilities of the presented model provide a possibility to predict changes in the material microstructure after SPD of materials with various chemical compositions.

The developed model was embedded into a computational code based on the Finite Element Method. New plasticity models were implemented as USERMAT FORTRAN subroutine for ANSYS commercial finite element software. Performed three-dimensional finite element modeling calculates the degree of strain inhomogeneity. The same analysis predicts microstructure formed within the material and gives a possibility to estimate different microstructural properties including the average aspect ratio of grains formed after the initial stages of MDF. Qualitatively the results of 3D modeling are repeating the results of the simplified 1D calculations displaying all the variety of the previously discussed phenomena. After the first pass of the MDF process, plastic strain accumulated in the central part of the deformed sample was calculated to be twice as big (~0.8) as comparing to strain evaluated supposing uniform strain distribution (~0.4). This fact is highly important and requires the corresponding corrections while processing and presenting experimental data for MDF.

A very interesting effect, predicted by the developed approach is the delay (for strains below 1) of grain refinement, while the size of dislocation cells is significantly reduced already for the first pass of MFD process. Also, the model was used to predict strain dependency of

fraction of triple junctions with number (0 to 3) of adjacent HAGBs. The received predictions can be verified experimentally and providing a much better understanding of mechanisms and processes constituting dynamic recrystallization in metals.

Acknowledgements

E.N. Borodin highly appreciates the financial support of EPSRC via grant EP/N026136/1 “Geometric Mechanics of Solids”. Vladimir Bratov declares no support from any scientific fund or program towards research presented here or preparation of this publication.

References

[1] T. Sakai, A. Belyakov, R. Kaibyshev, H. Miura, J.J. Jonas, Dynamic and post-dynamic recrystallization under hot, cold and severe plastic deformation conditions, Prog. Mater. Sci. 60 (2014) 130–207.
[2] A. Belyakov, T. Sakai, H. Miura, K. Tsuzaki, Grain refinement in copper under large strain deformation, Phil. Mag. A 81 (2001) 2629–2643.
[3] R.Z. Valiev, R.K. Islamgaliev, I.V. Alexandrov, Bulk nanostructured materials from severe plastic deformation, Prog. Mater. Sci. 45 (2000) 103–189.
[4] Y. Estrin, L.S. Tóth, Y. Bréchet, H.S. Kim, Modelling of the evolution of dislocation cell misorientation under severe plastic deformation, Mater. Sci. Forum 503 (2006) 675–680.
[5] Y. Estrin, L.S. Toth, A. Molinari, Y. Brechet, A dislocation- based model for all hardening stages in large strain deformation, Acta Mater. 46 (1998) 5509–5522.
[6] Y. Estrin, A. Vinogradov, Extreme grain refinement by severe plastic deformation: a wealth of challenging science, Acta Mater. 61 (2013) 782–817.
[7] M.J. Zehetbauer, Y.T. Zhu (Ed.), Bulk Nanostructured Materials, Willey-VCH, 2009.
[8] S. Yan, H. Yang, H. Li, X. Yao, A unified model for coupling constitutive behavior and micro-defects evolution of aluminum alloys under high-strain-rate deformation, Int. J. Plast. 85 (2016) 203–229.
[9] I. Sabirov, M.Yu. Murashkin, R.Z. Valiev, Nanostructured aluminium alloys produced by severe plastic deformation: new horizons in development, Mat. Sci. Eng. A 560 (2013) 1–24.
[10] M.P. Liu, H.J. Roven, M.Y. Murashkin, R.Z. Valiev, Structure and mechanical properties of nanostructured Al-Mg alloys processed by severe plastic deformation, J. Mater. Sci. 48 (2013) 4681–4688.
[11] P. Ghosh, O. Renk, R. Pippan, Microtexture analysis of restoration mechanisms during high pressure torsion of pure nickel, Materials Science Engineering A 684 (2017) 101–109.
[12] A.P. Zhilyaev, T.G. Langdon, Using high-pressure torsion for metal processing: fundamentals and applications, Prog. Mater. Sci. 53 (2008) 893–979.
[13] R.Z. Valiev, T.G. Langdon, Principles of equal-channel angular pressing as a processing tool for grain refinement, Prog. Mater. Sci. 51 (2006) 881–981.
[14] Sh.R. Bahadori, K. Dehghani, S.A.A.A. Mousavi, Comparison of microstructure and mechanical properties of pure copper processed by twist extrusion and equal channel angular pressing, Mater. Lett. 152 (2015) 48–52.
[15] C. Arnaud, F. Lecouturier, D. Mesguich, N. Ferreira, G. Chevallier, C. Estournès, A. Weibel, A. Peigney, C. Laurent, High strength–high conductivity nanostructured copper wires prepared by spark plasma sintering and room temperature severe plastic deformation, Mat. Sci. Eng. A 649 (2016) 209–213.
[16] S. Patala, J.K. Mason, C.A. Schuh, Improved representations of misorientation information for grain boundary science and engineering, Prog. Mater. Sci. 57 (2012) 1383–1425.
[17] M. Liu, T. Jiang, X. Xie, Q. Liu, X. Li, H.J. Roven, Microstructure evolution and dislocation configurations in nanostructured Al-Mg alloys processed by high pressure torsion, Trans. Nonferrous Metals Soc. China 24 (2014) 3848–3857.
[18] A. Mishra, B.K. Kad, F. Gregori, M.A. Meyers, Microstructural evolution in copper subjected to severe plastic deformation: experiments and analysis, Acta Mater. 55 (2007) 13–28.
[19] F. Roters, P. Eisenlohr, L. Hantcherli, D.D. Tjahjanto, T.R. Bieler, D. Raabe, Overview of constitutive laws, kinematics, homogenization and multiscale methods in crystal plasticity finite-element modeling: theory, experiments, applications, Acta Mater. 58 (2010) 1152–1211.
[20] A.V. Shutov, C.B. Silbermann, J. Ihlemann, Ductile damage model for metal forming simulations including refined description of void nucleation, Int. J. Plast. 71 (2015) 195–217.
[21] T. Horn, C.B. Silbermann, P. Frint, M.F.-X. Wagner, J. Ihlemann, Strain localization during equal-channel angular pressing analyzed by finite element simulations, Meta 8 (2018) 55.
[22] C.B. Silbermann, A.V. Shutov, J. Ihlemann, Modeling the evolution of dislocation populations under non-proportional loading, Int. J. Plast. 55 (2014) 58–79.
[23] S.C. Baik, Y. Estrin, H.S. Kim, R.J. Hellmig, Dislocation density-based modeling of deformation behavior of aluminium under equal channel angular pressing, Mater. Sci. Eng. A 351 (2003) 86–97.
[24] D.J. Lee, E.Y. Yoon, D. Ahn, B.H. Park, H.W. Park, L.J. Park, Y. Estrin, H.S. Kim, Dislocation density-based finite element analysis of large strain deformation behavior of copper under high-pressure torsion, Acta Mater. 76 (2014) 281–293.
[25] N.A. Enikeev, H.S. Kim, I.V. Alexandrov, Kinetic dislocation model of microstructure evolution during severe plastic deformation, Mater. Sci. Eng. A 460–461 (2007) 619–623.
[26] I.V. Alexandrov, R.G. Chembarisova, V.D. Sitdikov, Analysis of the deformation mechanisms in bulk ultrafine grained metallic materials, Mat. Sci. Eng. A 463 (2007) 27–35.
[27] A.A. Smolyakov, V.P. Solovyev, A.I. Korshunov, N.A. Enikeev, Three-dimensional numerical simulations of multi-pass equal-channel angular pressing by a variation difference method and comparison with experiment, Mat. Sci. Eng. A 493 (2008) 148–159.
[28] E. Cerri, P.P. De Marco, P. Leo, FEM and metallurgical analysis of modified 6082 aluminium alloys processed by multipass ECAP: Influence of material properties and different process settings on induced plastic strain, J. Mater. Process. Technol. 209 (2009) 1550–1564.
[29] P. Basavaraj, V.U. Chakkingal, T.S.P. Kumar, Effect of geometric parameters on strain, strain inhomogeneity and peak pressure in equal channel angular pressing – a study based on 3D finite element analysis, J. Manufact. Proc. 17 (2015) 88–97.
[30] V. Bratov, E.N. Borodin, Comparison of dislocation density based approaches for prediction of defect structure evolution in aluminium and copper processed by ECAP, Mat. Sci. Eng. A 631 (2015) 10–17.
[31] G.A. Malygin, Dislocation self-organization processes and crystal plasticity, Physics-Uspekhi 169 (1999) 979.
[32] A.E. Dudorov, A.E. Mayer, Equations of dislocation dynamics and kinetics at high rates of plastic deformation, Vestn. Chelyabinsk State Univ. Phys. 39 (2011) 12.
[33] K.S. Kumar, H. Van Swygenhoven, S. Suresh, Mechanical behavior of nanocrystalline metals and alloys, Acta Mater. 51 (2003) 5743–5774.
[34] A.E. Mayer, K.V. Khishchenko, P.R. Levashov, P.N. Mayer, Modeling of plasticity and fracture of metals at shock loading, Appl. Phys. J. 113 (2013) 193,508.
[35] C. Kittel, Introduction to Solid State Physics, Wiley Sons, New York, 2005.
[36] P. Rosakis, A.J. Rosakis, G. Ravichandran, J. Hodowany, A thermodynamic internal variable model for the partition of plastic work into heat and stored energy in metals, J. Mech. Phys. Solids 48 (2000) 58–607.
[37] E.I. Galindo-Nava, P.E.J. Rivera-Dıaz-del-Castillo, A thermodynamic theory for dislocation cell formation and misorientation in metals, Acta Mater. 60 (2012) 4370–4378.
[38] A. Vinogradov, Mechanical properties of ultrafine-grained metals: new challenges and perspectives, Adv. Eng. Mater. 17 (12) (2015) 1710–1722.
[39] M.W. Guinan, D.J. Steinberg, Pressure and temperature derivatives of the isotropic polycrystalline shear modulus for 65 elements, J. Phys. Chem. Solids 35 (1974) 1501–1512.
[40] H. Ding, N. Shen, Y. Shin, Predictive modeling of grain refinement during multi-pass cold rolling, J. Mater. Process. Technol. 212 (2012) 1003–1013.
[41] M.A. Meyers, K.K. Chawla, Mechanical Behavior of Materials, Cambridge University Press, New York, 2009.
[42] E.V. Kozlov, A.N. Zhdanov, N.A. Popova, E.E. Pekarskaya, N.A. Koneva, Subgrain structure and internal stress fields in UFG materials: problem of Hall–Petch relation, Mater. Sci. Eng. A 387–389 (2004) 789–794.
[43] V. Shterner, A. Molotnikov, I. Timokhina, Y. Estrin, H. Beladi, A constitutive model of the deformation behaviour of twinning induced plasticity (TWIP) steel at different temperatures, Mater. Sci. Eng. A 613 (2014) 224–231.
[44] H. Liu, W. Pantleon, L. Mishnaevsky, Non-equilibrium grain boundaries in titanium nanostructured by severe plastic deformation: computational study of sources of material strengthening, Comput. Mater. Sci. 83 (2014) 318–330.
[45] P.W.J. Mckenzie, R. Lapovok, Y. Estrin, The influence of back pressure on ECAP processed AA 6016: modeling and experiment, Acta Mater. 55 (2007) 2985–2993.
[46] D. Rittel, S. Osovski, Dynamic failure by adiabatic shear banding, Int. J. Fract. 162 (1) (2010) 177–185.
[47] I.V. Alexandrov, A.A. Dubravina, H.S. Kim, Nanostructure formation in copper subjected to high pressure torsion, Defect Diffus Forum 208–209 (2002) 229–232.
[48] T. Ungar, M. Zehetbauer, I.V. Stage, Work-hardening in cell forming materials. 2. A new mechanism, Scr. Mater. 35 (1996) 1467–1473.
[49] E.N. Borodin, A.E. Mayer, P.N. Mayer, Grain size dependence of the yield stress for metals at quasistatic and dynamic loadings, Proc. 13th International Conference on Fracture June 16–21, Beijing, China, 2013.
[50] N.A. Koneva, E.V. Kozlov, Deformation-induced ordering of dislocation structures, Mater. Sci. Eng. A 387–389 (2004) 64–66.
[51] M.A. Meyers, V.F. Nesterenko, J.C. La Salvia, Y.B. Xu, Q. Xue, Observation and modeling of dynamic recrystallization in high-strain, high-strain rate deformation of metals, J. Phys. IV France 10 (2000) 51–56.
[52] J.P. Hirth, J. Lothe, Theory of Dislocations, Wiley Sons, New York, 1982.
[53] R. Lapovok, F.H. Dalla Torre, J. Sandlin, C.H.J. Davies, E.V. Pereloma, P.F. Thomson, Y. Estrin, Gradient plasticity constitutive model reflecting the ultrafine micro-structure scale: The case of severely deformed copper, J. Mech. Phys. Solids 53 (2005) 729–747.
[54] E.I. Galindo-Nava, P.E.J. Rivera-Diaz-del-Castillo, A thermostatistical theory of low and high temperature deformation in metals, Mater. Sci. Eng. A 543 (2012) 110–116.
[55] E.I. Galindo-Nava, J. Sietsma, P.E.J. Rivera-Diaz-del-Castillo, Dislocation annihilation in plastic deformation: II. Kocks-Mecking analysis, Acta Mater. 60 (2012) 2615–2624.
[56] R.D. Doherty, D.A. Hughes, F.J. Humphreys, J.J. Jonas, D.J. Jensen, M.E. Kassner, W.E. King, T.R. McNelley, H.J. McQueen, A.D. Rollett, Current issues in recrystallization: a review, Mater. Sci. Eng. A 238 (1997) 219–274.
[57] M. Li, T. Xu, Topological and atomic scale characterization of grain boundary networks in polycrystalline and nanocrystalline materials, Prog. Mater. Sci. 56 (2011) 864–899.
[58] K. Yvell, T.M. Grehk, G. Engberg, Microstructure characterization of 316 L deformed at high strain rates using EBSD, Mater. Charact. 122 (2016) 14–21.

[59] A.A. Nazarov, N.A. Enikeev, A.E. Romanov, T.S. Orlova, I.V. Alexandrov, I.J. Beyerlein, R.Z. Valiev, Analysis of substructure evolution during simple shear of polycrystals by means of a combined viscoplastic self-consistent and disclination modeling approach, Acta Mater. 54 (2006) 985–995.
[60] A. Morozova, R. Kaibyshev, Grain refinement and strengthening of a Cu–0.1Cr–0.06Zr alloy subjected to equal channel angular pressing, Philos. Mag. (2017) 1–24.
[61] R.Z. Valiev, V.Y. Gertsman, O.A. Kaibyshev, Grain boundary structure and properties under external influences, Phys. Status Solidi 97 (1) (1986) 11–51.
[62] E.A. Rzhavtsev, M.Yu. Gutkin, The dynamics of dislocation wall generation in metals and alloys under shock loading, Scr. Mater. 100 (2015) 102–105.
[63] J. Xu, J. Li, D. Shan, B. Guo, Microstructural evolution and micro/mesodeformation behaviour in pure copper processed by equal-channel angular pressing, 664 (2016) 114–125.
[64] U.F. Kocks, H. Mecking, Physics and phenomenology of strain hardening: the FCC case, Prog. Mater. Sci. 48 (2003) 171–273.
[65] M. Frary, C.A. Schuh, Percolation and statistical properties of low- and high-angle interface networks in polycrystalline ensembles, Phys. Rev. B 69 (2004) 134,115.
[66] I.A. Ovid'ko, A.G. Sheinerman, E.C. Aifantis, Stress-driven migration of grain boundaries and fracture processes in nanocrystalline ceramics and metals, Acta Mater. 56 (2008) 2718–2727.
[67] C.B. Silbermann, J. Ihlemann, Kinematic assumptions and their consequences on the structure of field equations in continuum dislocation theory, IOP Conference Series: Materials Science and Engineering 118 (2016) 1–11.
[68] M. Wang, L. Huang, W. Liu, Y. Ma, B. Huang, Influence of cumulative strain on microstructure and mechanical properties of multi-directional forged 2A14 aluminum alloy, Mat. Sci. Eng. A 674 (2016) 40–51.
[69] A.I. Rudskoy, Nanostrukturirovannye metallicheskie materialy (Nanostructured metallic materials). Saint Petersburg : Nauka, (2011), p. 297.
[70] Y. Estrin, H.-B. Muhlhaus, From micro- to macroscale: gradient models of plasticity, in: W.Y.D. Yen, P. Broadbridge, J.M. Steiner (Eds.), Australian Engineering Mathematics Conference. Sydney, 1996, pp. 161–165.
[71] Y. Estrin, A. Molotnikov, C.H.J. Davies, R. Lapovok, Strain gradient plasticity modelling of high-pressure torsion, Journal of the Mechanics and Physics of Solids 56 (2008) 1186–1202.